EPJ Web of Conferences **61**, 03004 (2013)
DOI: 10.1051/epjconf/ 20136103004

Spectra and fast multi-wavelength variability of compact jets powered by internal shocks.

Julien Malzac[1,2,a]

[1] *Université de Toulouse; UPS-OMP; IRAP; Toulouse, France,*

[2] *CNRS; IRAP; 9 Av. colonel Roche, BP 44346, F-31028 Toulouse cedex 4, France*

Abstract. The emission of steady compact jets observed in the hard spectral state of X-ray binaries is likely to be powered by internal shocks caused by fluctuations of the outflow velocity. The dynamics of the internal shocks and the resulting spectral energy distribution (SED) of the jet is very sensitive to the shape of the Power Spectral Density (PSD) of the fluctuations of the jet Lorentz factor. I used both Monte-Carlo simulations and semi-analytical methods to investigate this dependence. It turns out that Lorentz factor fluctuations injected at the base of the jet with a flicker noise power spectrum (i.e. P(f) 1/f) naturally produce the canonical flat SED observed from radio to IR band in X-ray binary systems in the hard state. This model also predicts a strong, wavelength dependent, variability that resembles the observed one. In particular, strong sub-second variability is predicted in the infrared and optical bands. The complex timing correlations observed between the IR/optical light curves and the X-rays can then be used to probe the accretion/ejection connection on short time-scales.

1 Introduction

Steady compact jets are probably the most common form of jets in X-ray binaries. They appear to be present in all black hole and neutron star binaries when in the hard X-ray spectral state. They have an approximatively flat Spectral Energy Distribution (SED) extending from the radio to the mid-IR (e.g. Fender et al. 2000; Corbel & Fender 2002; Chaty et al. 2003; Migliari et al. 2010). These flat spectra are usually ascribed to self-absorbed synchrotron emission from conical compact jets (Blandford & Königl 1979) under the assumption of continuous energy replenishment of the adiabatic losses. The compensation of these energy losses is crucial for maintaining this specific spectral shape (Kaiser 2006).

Internal shocks provide a possible mechanism to compensate the adiabatic losses by dissipating energy and accelerating particles at large distance from the black hole. Internal shocks caused by fluctuations of the outflow velocity are indeed widely believed to power the multi-wavelength emission of jetted sources such as γ-ray bursts (Rees & Meszaros 1994; Daigne & Moscovitch 1998), active galactic nuclei (Rees 1978; Spada et al. 2001), or microquasars (Kaiser, Sunyaev & Spruit 2000; Jamil et al. 2010). Internal shocks models usually assume that the jet can be discretised into homogeneous ejectas. Those ejectas are injected at the base of the jet with variable velocities and then propagate along the jet. At some point, the fastest fluctuations start catching up and merging with slower ones. This leads to shocks in which a fraction of the bulk kinetic velocity of the shells is converted into internal energy. Part of the dissipated energy goes into particles acceleration, leading to synchrotron and also, possibly, inverse Compton emission. Recently, however, Jamil et al. (2010) developed an internal shock model for the emission of jets in X-ray binaries, and concluded that energy dissipation through internal shocks only is not enough to produce a flat SED. Nevertheless, most studies of the internal shock model so far, including that of Jamil et al. (2010), have implicitly assumed that the Fourier Power Spectral Density (PSD) of the velocity fluctuations injected at the base of the jet is flat (i.e. white noise). In fact, the energy dissipation profile of the internal shocks is very sensitive to the shape of the PSD of the velocity fluctuations. Indeed, let us consider a fluctuation of the jet velocity of amplitude Δv occuring on a time scale Δt. This leads to the formation of a shock at a downstream distance $z_s \propto \Delta t/\Delta v$. In this shock the fraction of the kinetic energy converted into internal energy will be larger for larger Δv. From these simple considerations we see that the distribution of the velocity fluctuation amplitudes over their time scales (i.e. the PSD) is going to determine where and in which amount the energy of the internal shocks is deposited. In this paper we investigate different types of fluctuations.

2 Spectral energy distributions from jet Lorentz factor fluctuations with a power-law PSD

Instead of using white noise we use a more general model and assume that the PSD of the Lorentz factor of the jet

[a] e-mail: Julien.malzac@irap.omp.eu

Article available at http://www.epj-conferences.org or http://dx.doi.org/10.1051/epjconf/20136103004

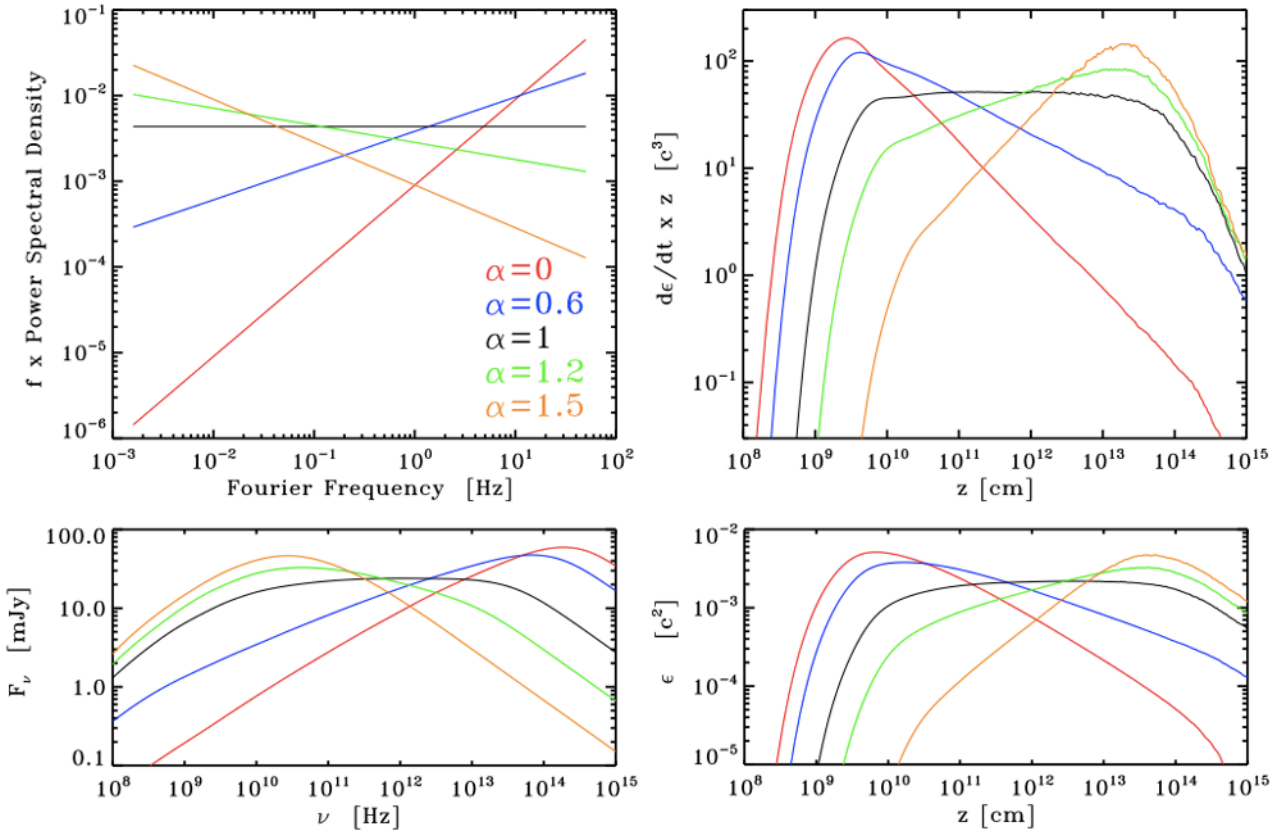

Figure 1. Simulation of the internal shock model with a power-law PSD of the Lorentz factor fluctuations ($P(f) \propto f^{-\alpha}$). The top left panel shows the the shape of the injected PSDs, for the indicated values of the α index. Then moving clockwise other panels show the time averaged dissipation profile along the jet, the specific energy profile and the jet SED respectively. The SEDs are calculated for an inclination angle of 40 degrees and a distance to the source of 2 Kpc

has a power-law shape with index α: $P(f) \propto f^{-\alpha}$. I used a code similar to that of Jamil et al. (2010) to explore the dependence of the photon spectrum on α. Fig 1 shows that the dissipation profile along the jet and the profile of the specific energy of the flow are very sensitive to α. For larger α the fluctuations of the Lorentz factor have, on average, longer time-scales and therefore more dissipation occurs at larger distances from the black hole. For the case $\alpha = 0$ (i.e. white noise) we can see that most of the dissipation occurs very close to the black hole and then the dissipation rate decrease very quickly (like $z^{-5/3}$). As a consequence the specific energy profile is steep and therefore the adiabatic losses are not compensated. The photon spectrum is strongly inverted, with a slope $\simeq 0.65$ i.e more inverted than most of the observed spectra, this is in aggreement with the conclusions of Jamil et al. (2010). On the other hand, one can see from Fig. 1 that for $\alpha = 1$ (i.e. flicker noise) the dissipation profile scales like z^{-1} and the specific energy profile is flat. In other words, the internal shocks compensate exactly for the adiabatic losses. As result the SED is flat over a wide range of photon frequencies. In fact, this result can also be obtained analytically (Malzac 2013). The case of flicker noise fluctuations of the jet Lorentz factor may therefore be relevant to the observations of compact jets.

3 Flicker noise fluctuations of the jet Lorentz factor

In fact flicker noise fluctuations are not unexpected. Indeed, if the jet is launched by the accretion disc, the variability of the jet Lorentz factor must be related to that of the accretion disc. And we know, both from theory (see e.g. Lyubarskii 1995) and from observations (see e.g. Gilfanov & Arefiev 2005) that accretion discs tend to generate flicker noise variability. Also, the highest and lowest frequencies of variability f_0 and f_1 must relate to time scales of the accretion flow. In the simulations show in Fig. 1, we choose $f_1 = 1.6 \times 10^{-3}$ Hz and $f_0 = 50$ Hz corresponding to the Keplerian timescale at 10^4 R_g and 10 R_g from a 10 $M_\odot$ black hole respectively. We also assumed an average Lorentz factor of 2 varying with fractional rms amplitude of 30 percent, i.e. comparable to that observed in the X-ray variability of black hole binaries in the hard state. With these parameters, the dissipations starts at a distance of a few 10^9 cm. This is comparable to the distance of $\sim 10^3 R_g$ inferred in Cyg X-1 both by the modelling the of SED (Zdziarski et al. 2012), and that of the orbital modulation of the radio emission (Zdziarski 2012). Our choice for the longest timescale of the injected fluctuations implies that significant dissipation occurs up to a distance of a about 10^{14} cm which is roughly comparable to the ex-

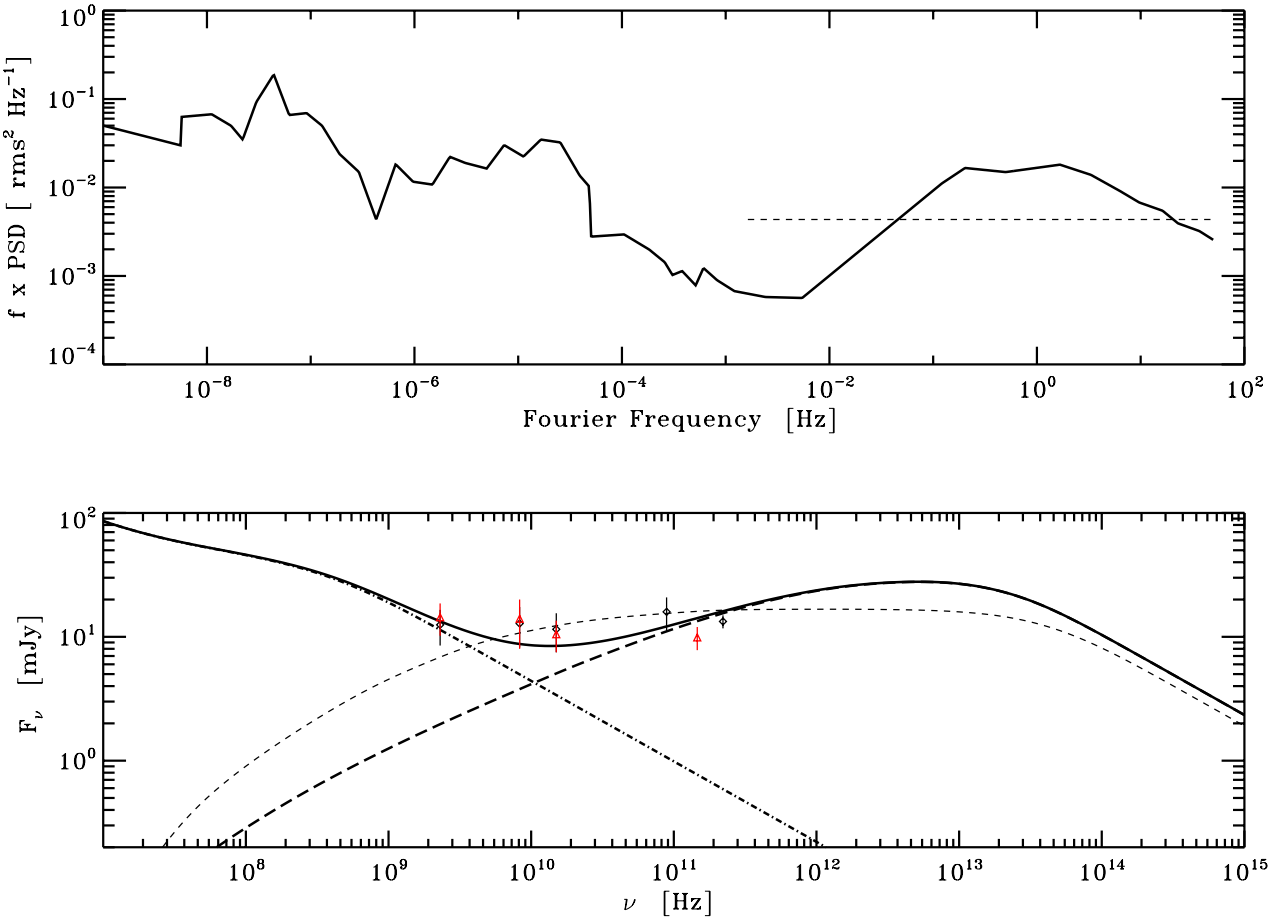

Figure 2. Top the observed X-ray PSD of Cyg X-1. Bottom: simulated jet SED obtained assuming that the jet Lorentz factor fluctuations have exactly the PSD as the X-ray flux.The triangle and diamonds are measurements of the radio-mm SED obtained by Fender et al. Dashed and dot dashed curves show the contribution from high frequency Lorentzians and the power-like components of the Fourrier PSD respectively. In both panels the thin dashed curves show the result of the fiducialsimulation with flicker noise fluctuations of the Jet Lorentz factor.

tension of the radio jet of Cyg X-1 in the VLBA images of Stirling et al. (2001). These authors also constrain the jet opening angle of Cyg X-1 to be small $\phi < 2^o$. This implies that the radius of the jet at the base of the emitting region is at most of a few 10^8 cm. We assumed that the jet power is of the oder of a few percent of the Eddington luminosity L_E as infered in Cyg X- 1 (Gallo et al. 2005). This implies an equipartition magnetic field at the base of the emitting region, of the order of 10^4 gauss. These estimates for the jet radius and magnetic field at the base of the dissipation region are comparable to the values inferred in Cyg X-1 (Zdziarski et al. 2012), GX 339-4 (Gandhi et al. 2011) and XTE J1550-564 (Chaty et al. 2011). The SEDs of Fig. 1 are evaluated assuming that the synchrotron emitting electrons have a power law energy distribution $n(\gamma_e) \propto \gamma_e^{-2.3}$ for electrons Lorentz factors, γ_e, in the range 1–10^6. This estimate is consistent with the flux observed in bright hard states (e.g. at $\simeq$ 2 kpc, Cyg X-1 has an average radio flux of 15 mJ at 15 GHz). The turnover frequency appears in the mid-infrared $\nu_t \simeq 2 \times 10^{13}$ Hz, in agreement with the observations of Cyg X-1 (Rahoui et al. 2011) or GX 339-4 (Gandhi et al. 2011): Finally the model predicts that the emission should decrease significantly at frequencies below $\nu_s \sim 1$ GHz. The specific value of ν_s depends on f_1 and this is something that can be investigated in the near future with LOFAR.

3.1 Are the jet Lorentz factor fluctuations related to the X-ray variability ?

As discussed above, the fluctuations of the jet Lorentz factor are likely to be related to the variability of the accretion flow. In fact, this variability can be traced directly in the the X-ray light curves of X-ray binaries. Those sources indeed exhibit a strong variability over a very broad range of time scales. Although this variability is close to flicker noise, it appears to be more complex (see top panel of Fig. 2). At very low Fourier frequencies (in the range 10^{-8}–10^{-3} Hz) the power spectrum of persistent sources has a power-law shape with $\alpha \simeq 1.3$ (Reig

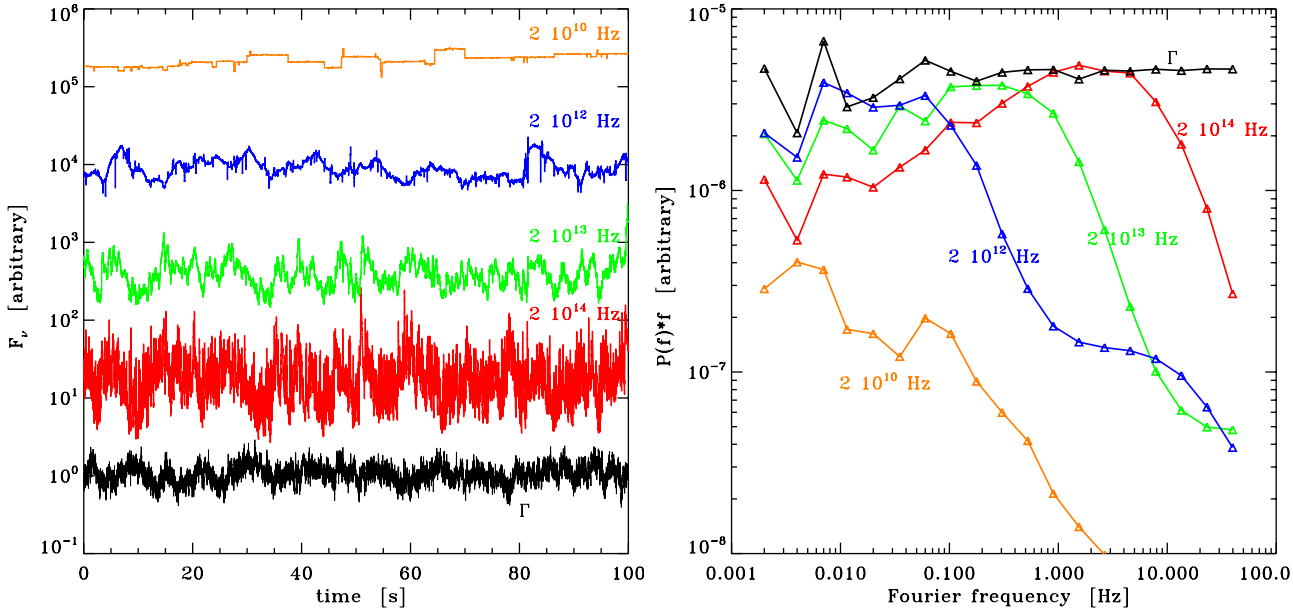

Figure 3. Synthetic light curves (left, rescaled) and power spectra at various indicated frequencies resulting from the simulation with $\alpha = 0$. The injected fluctuations of the Lorentz factor are also shown.

et al. 2002; Gilfanov 2010), while in the hard state and at shorter time scales the the variability is dominated by a band limited noise that is well described in terms of 4-5 broad Lorentzians (e.g. Nowak 2000; van der Klis 2006).

The observed X-ray PSD of Cygnus X-1 was extracted from the figure 6 of Gilfanov (2010) in the range 10^{-9}-50 Hz, and used as input for the Lorentz factors fluctuations. It is worth noting that not only the shape but also the normalisation of the PSD is used as input of the internal shock model. The other parameters of the model remain the same.

As can be seen from Fig 2, the observed PSD covers a very wide range of frequencies, corresponding to about 11 orders of magnitudes. In order to simulate all the time-scales we would need to generate a time-series of Lorentz factor fluctuations with a resolution of a few tenth of milliseconds and of duration of about 30 years. Due to computer memory limitations and available computing time, it was unfortunately not possible to generate such a time series containing about a hundred billions of elements. Instead, we can combine the results of two simulations dealing with different time-scales. The first one we use the observed PSD of Cyg X-1 only beetween 3×10^{-3} Hz and 10^2 Hz and simulate the evolution of the system during 10^5 s after the first ejection. This simulation corresponds to the case in which only the high frequency band-limited noise (Lorentzians) contribute to the variability of the jet Lorentz factor. The result is shown in dashed curves in Fig. 2.The second simulation uses the observed X-ray PSD of Cygnus X-1 in the frequency range 10^{-9} to 3×10^{-3}. This simulation corresponds to the contribution of the low frequency power-law like component and is shown in dot-dashed curves in Fig 2.The quantities are averaged from 10^3 to 10^9 s after the first ejection.

The drastically different time-scales of the two components lead to energy dissipation in two distinct region of the jet. The high frequency band limited noise component produces a SED that is quite inverted in the radio band, the SED peaks around 10^{13} Hz and the break in the NIR is correctly produced. The low frequency power-law like noise component produces dissipation mostly at large distances (around 10^{12} R_G). As a consequence of the large scales involved, the SED of the low Fourier frequency component is optically thin above 1 GHz. Since the two variability components have effects at very different distances they are mostly decoupled. A good approximation of the simulation taking into account the full range of variability time scales can be obtained simply, by summing their respective contributions. The result is shown by the full curve in the bottom panel of Fig. 2. As can be seen, the contribution of the low and high frequency variability components combine to produce the remarkably flat SED observed in Cygnus X-1.

Fig. 2 also shows a comparison with the fiducial flicker noise model discussed in Section 3. As can be seen on the top panel the X-ray PSD contains less noise than the flicker noise model at highest frequencies and therefore the the dissipation starts at larger distances. However between 4×10^{-2} and 20 Hz, the X-ray PSD amplitude is larger and the dissipation rate becomes larger than that of the flicker noise model between 10^4 and 10^6 R_G. At lower frequencies the X-ray PSD present less power than the flicker noise, however the X-ray power spectrum increases toward low frequencies as it becomes dominated by the low frequency power-law component, while in the flicker-noise model there is no noise below 1.6×10^{-3} Hz. This causes the main difference between the two models: if the Lorentz factor fluctuations have a low Fourier fre-

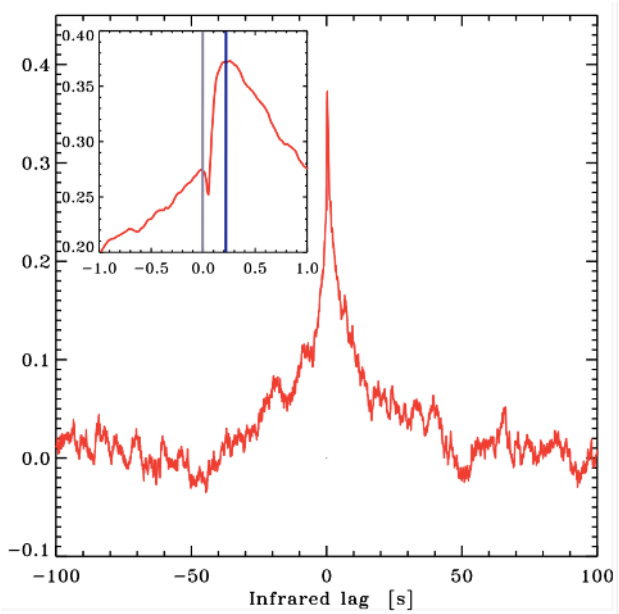

Figure 4. Cross correlation function of $1/\Gamma(t)$ and predicted IR flux from the fiducial flicker noise simulation

quency component similar to that in the X-ray PSD, the low frequency cut-off predicted by the pure flicker noise model does not exist.

4 Timing

An interesting feature of the internal shock model is that it naturally predicts strong variability of the the jet emission. Figure 3 shows sample light curves and power spectra obtained from the simulation with $\alpha = 1$. The jet behaves like a low-pass filter. As the shells of plasma travel down the jet, colliding and merging with each other, the highest frequency velocity fluctuations are gradually damped and the size of the emitting region increases. The jet is strongly variable in the optical and IR bands originating primarily from the base of the emitting region and become less and less variable at longer frequencies produced at larger distances from the black hole. The observations also show significant flickering in the Infrared and optical band (Kanbach et al. 2001; Casella et al. 2010; Gandhi et al. 2010). At least part of this fast IR/optical variability is likely to arise from the jet, possibly through internal shocks. Another interesting property of the observed variability is the existence of correlations with the fast X-ray variability originating from the accretion flow. In particular, Casella et al. (2010) measured de cross-correlation function of the X-ray and IR light curves and found significant correlation between the two bands with the infrared photons lagging behind the X-rays by about 100 ms. At this stage the present internal shock model does not describe how the fluctuations of the Lorentz factor may be related to the X-ray fluctuations. Nevertheless, we can make simple guesses. Fig. 4 shows the results obtained if one assumes that the X-ray flux scales like $1/\Gamma(t)$. This case may correspond to a situation in which both the the jet and X-ray emission tap their energy from a single energy reservoir and are anti-correlated (Malzac, Merloni & Fabian 2004). Alternatively, this could also correspond to a situation in which the jet kinetic power is a constant and the Lorentz factor fluctuations are related to fluctuations of the matter density in the innermost part of the accretion. This would induce fluctuations of the jet mass loading, causing a reduction of the Lorentz factor when the ejected shells are more massive. At the same time the X-ray flux should scale approximately like the square of the accretion flow density. Causing the jet Lorentz factor and X-ray flux to be anti-correlated. In any case, Fig. 4, shows a cross correlation function that is very similar to that observed by Casella et al. (2010). As can be seen from the inset of Fig 4, the simulated IR light curves lags by about 200 ms behind the X-rays.

5 Conclusion

Internal shocks driven by (approximately) flicker noise fluctuations can therefore produce not only the flat SED of compact jets in X-ray binaries, but also other properties such as the flux amplitude or the location of the break frequency and perhaps also the presence of IR/X-ray lags. The model also predicts strong multi-wavelength variability that appear to be similar to that observed. These results also suggest a relation between the X-ray timing properties and the shape of the radio to IR SED, that remains to be investigated.

References

[1] Blandford R. D., Königl A., 1979, ApJ, 232, 34
[2] Casella P., et al., 2010, MNRAS, 404, L21
[3] Chaty S., et al., 2003, MNRAS, 346, 689
[4] Chaty S., Dubus G., Raichoor A., 2011, A&A, 529, A3
[5] Corbel S., Fender R. P., 2002, ApJ, 573, L35
[6] Daigne F., Mochkovitch R., 1998, MNRAS, 296, 275
[7] Fender R. P., et al., 2000, MNRAS, 312, 853
[8] Gallo E., et al. , 2005, Natur, 436, 819
[9] Gandhi P., et al., 2010, MNRAS, 407, 2166
[10] Gandhi P., et al., 2011, ApJ, 740, L13
[11] Gilfanov M., 2010, LNP, 794, 17
[12] Gilfanov M., Arefiev V., 2005, astro, arXiv:astro-ph/0501215
[13] Jamil O., Fender R. P., Kaiser C. R., 2010, MNRAS, 401, 394
[14] Kaiser C. R., Sunyaev R., Spruit H. C., 2000, A&A, 356, 975
[15] Kaiser C. R., 2006, MNRAS, 367, 1083
[16] Kanbach G., Straubmeier C., Spruit H. C., Belloni T., 2001, Natur, 414, 180
[17] Lyubarskii Y. E., 1997, MNRAS, 292, 679
[18] Malzac J., 2013, MNRAS, 429, L20
[19] Migliari S., Miller-Jones J. C. A., Russell D. M., 2011, MNRAS, 415, 2407

[20] Nowak M. A., 2000, MNRAS, 318, 361
[21] Rahoui F., et al., 2011, ApJ, 736, 63
[22] Reig P., Papadakis I., Kylafis N. D., 2002, A&A, 383, 202
[23] Rees M. J., 1978, MNRAS, 184, 61P
[24] Rees M. J., Meszaros P., 1994, ApJ, 430, L93
[25] van der Klis M., in Compact stellar X-ray sources, Lewin & van der Klis (eds), Cambridge University Press, 2006, arXiv:astro-ph/0410551
[26] Spada M., Ghisellini G., Lazzati D., Celotti A., 2001, MNRAS, 325, 1559
[28] Stirling A. M., et al., 2001, MNRAS, 327, 1273
[28] Stirling A. M., et al., 2001, MNRAS, 327, 1273
[29] Zdziarski A. A., 2012, MNRAS, 422, 1750
[30] Zdziarski A. A., Lubiński P., Sikora M., 2012, MNRAS, 2816